Influence of electric fields on metal self-diffusion barriers and its consequences on dendrite growth in batteries

Markus Jäckle and Axel Groß

Institute of Theoretical Chemistry, Ulm University, 89069 Ulm, Germany and

Helmholtz Institut Ulm (HIU) Electrochemical Energy Storage, 89069 Ulm, Germany

(Dated: October 24, 2019)

Abstract

Based on the results of periodic density functional theory calculations we have recently proposed that the height of self-diffusion barriers can serve as a descriptor for dendrite growth in batteries [Energy Environ. Sci 11, 3400 (2018)]. However, in the determination of the self-diffusion barriers, the electrochemical environment has not been taken into account. Still, due to the presence of electrical double layers at electrode/electrolyte interfaces, strong electric fields can be present close to the interfacial region. In a first step towards including the electrochemical environment, we have calculated barriers for terrace- and across-step self-diffusion processes on lithium and magnesium surfaces in the presence of electric fields. Our results yield a negligible influence of electric fields on self-diffusion barriers which we explain by the good screening properties of metals.

I.   INTRODUCTION

Our current energy supply is still dominated by fossil resources.[1,2] Because of the harmful environmental impact and the associated economical costs, a change towards renewable energy generation is needed[3–6]. However, due to the volatility of renewable sources such as wind and sunlight, efficient storage schemes such as battery storage systems are needed[7–9]. Furthermore, batteries also provide efficient energy storage in portable electronic devices, power tools and electromobility.

In spite of the significant improvement in battery technology in the last decades, there are still severe issues as far as battery performance is concerned, but also with respect to sustainability and safety aspects. As one of the most severe hazards the growth of dendrites has been identified[10–13]. Their formation can lead to short-circuits and in combination with a flammable electrolyte to highly exothermic reactions of the electrolyte called 'thermal runaways', which eventually can cause battery fires[14,15]. In addition, upon fracture dendrites cause a loss of anode material, the so called 'dead lithium'.[10,12,13]

Recently, we have shown that self-diffusion barriers can serve as a descriptor for the occurrence of dendrites[16–18]. This concept is based on the notion that diffusion generally tends to make inhomogeneities smooth[19] and means that the height of diffusion barriers is correlated to the tendency of a material to exhibit dendrite growth. These self-diffusion barriers have been derived from periodic density functional theory (DFT) calculations, in which, however, the electrochemical environment has not been taken into account.

At electrochemical interfaces, typically electric double layers (EDL) form, mainly resulting from ions that are attracted to charged electrodes and accumulate at the interface[20–28]. One of the consequences of the presence of the EDL is the creation of strong electric fields.[28,29] It has been shown that generated electric fields may influence the adsorption- and activation energies on metal surfaces,[30–32], the line tension of steps on surfaces[33], and the orientation of molecules on surfaces[34]. Furthermore, the roles of electric fields in catalysis has just recently been reviewed[35]. On the other hand, for the dissociation of oxygen on Pt(111) only a rather small increase in the dissociation barrier has been calculated for positive fields,[31] and the activation energy of desorption of cesium on tungsten has been observed to marginally decrease upon applying a negative electric field.[30]

As far as batteries are concerned, it has been shown that high current densities speed

up lithium dendrite growth,[14,15,36] and can even lead to magnesium dendrite growth[37,38]. Typically it has been assumed that heterogeneous deposition caused by large polarizations and strong electric fields tends to induce dendrite nucleation[36], however, most models of dendrite growth are not element-specific[19,39] and are thus not able to explain why, e.g., lithium tends to exhibit dendrite growth and magnesium not. The effect of electric fields with respect to dendrite growth has been linked to the direction of lithium fibre growth,[15,40], and to directed lithium deposition towards tips[13,15,41]. However, for bush-like lithium growth in $LiPF_6$ solutions no prefered growth direction was found,[42] also growth modes based on insertion at defects have been observed. Consequently the effect of electric fields on the growth direction ist still being debated[43].

Hence the effect of electric fields on the growth of dendrites at the electrode-electrolyte interfaces is still unclear. In this study, we first address the influence of externally applied electric fields on the self-diffusion behavior of lithium, magnesium, and also silver based on periodic DFT calculations, and then discuss the consequence of our findings on the growth of dendrites in batteries.

II. THEORETICAL BACKGROUND

Periodic density functional theory (DFT) calculations have been performed using the Vienna Ab initio Simulation Package (VASP).[44,45] Exchange-correlation effects have been accounted for within the generalized gradient approximation (GGA) employing the functional of Perdew, Burke, and Ernzerhof (PBE).[46] The core electrons are represented by projector augmented wave (PAW) pseudopotentials[47] as supplied in VASP[48] with a cutoff energy of 500 eV for lithium, and magnesium based systems, and 300 eV for the silver based system. We have chosen these values which are larger than the VASP default values in order to avoid any artifacts in the calculations including an explicit electric field. Up to a $7 \times 7 \times 1$ gamma-centered k-point grid was used ensuring convergence for the integration over the first Brillouin zone. In the calculations, the two uppermost layers were relaxed. The relaxation in the calculations has been performed until the forces were smaller than 10^{-3} eV and both the total free energy change and the band structure energy change were smaller than 10^{-6} eV.

In order to explicitly include electric fields in the calculations, we used the implementation

of electric fields in VASP as first introduced by Neugebauer and Scheffler,[49] and improved by Feibelman[50]. In this method, an artificial planar dipole layer is introduced and placed in the vacuum region exactly between the slab and its periodic image. In the calculations where asymmetric slabs have been used, a surface dipole-moment correction had been included,[49] in order to avoid the extra electric field due to the different dipole layers in this case.

Thus the dependence of the diffusion barriers on the electric field could be directly derived from the DFT calculations via

$$E_{act,DFT}(\vec{E}) = E_{TS}(\vec{E}) - E_{IS}(\vec{E}) \ , \tag{1}$$

where TS and IS denote the transition state (TS) and initial state (IS) of the diffusion path, respectively. It should be noted, however, that the SCF convergence of the Kohn-Sham calculations including an explicit electric field is severely slowed down compared to the field-free case, which makes these calculations numerically rather demanding.

In addition, we also used a first-order pertubation theory expression derived by Giesen et al.[51] for the diffusion barrier of a particle on a surface in the presence of an electric field,

$$E_{act}(\phi) = E_{act}^0 - (\mu_{TS} - \mu_{IS}) \cdot \frac{\sigma_0(\phi)}{\epsilon_0} \ , \tag{2}$$

where $E_{act}(\phi)$ is the diffusion barrier in dependence of the electrode potential ϕ, E_{act}^0 is the diffusion barrier in a field-free environment, $(\mu_{TS} - \mu_{IS})$ is the difference of the dipole moments perpendicular to the surface in the TS and in the IS in a field-free environment, and $\frac{\sigma_0(\phi)}{\epsilon_0}$ is the macroscopic charge density σ divided by the electric constant ϵ_0.

As already stated by Giesen et al.,[51] the correction term can be interpreted as the electrostatic energy of a dipole in an electric field $|\vec{E}| = \sigma_0(\phi)/\epsilon_0$, perpendicular to the surface. Inserting this into Eq. 2 yields

$$E_{act}(|\vec{E}|) = E_{act}^0 - (\mu_{TS} - \mu_{IS}) \cdot |\vec{E}| \ , \tag{3}$$

which can be regarded as being equivalent to a first-order Stark effect.[31]

However, the explicit determination of surface dipole moments can be quite cumbersome[52]. Still, in periodic calculations the dipole moment change per unit area can be

directly related to the corresponding change in the work function Φ according to [53]

$$\frac{\Delta\mu_0}{A_s} = \Delta\Phi\left(-\frac{\epsilon_0}{e_0}\right) \tag{4}$$

where A_s is the size of the surface unit cell. By inserting Eq. 4 into Eq. 3 one arrives at

$$E_{act}(|\vec{E}|) = E_{act}^0 + (\Phi_{TS} - \Phi_{IS})\frac{\epsilon_0}{e_0}\,A_s \cdot |\vec{E}| \;, \tag{5}$$

where Φ_{TS} and Φ_{IS} are the work functions associated with the transition and the initial state, respectively, of the diffusion event. This formula has been used to predict the change in the diffusion barrier as a function of the applied electric field.

III. RESULTS AND DISCUSSION

Selecting Li(100) as a test case, in Fig. 1 we first check the convergence of our results with respect to the size of the surface unit cell and the slab thickness using mainly the first-order expression (5) to derive the field-dependence of the diffusion barriers. Interestingly enough, the sign of the field-dependence changes when going from a 2×2 surface unit cell to a 4×4 cell. Obviously, in the 2×2 unit cell the diffusing atoms are so close to each other that there are significant depolarization effects that lead to an erroneous reverse field dependence. For a 5×5 unit cell (not shown in Fig. 1a), the work function change is hardly changed any more so that the 4×4 cell is apparently sufficiently large to avoid any substantial lateral interaction between the diffusing atoms.

The DFT calculations with the explicit electric field yield a field dependence that is somewhat smaller than the first-order expression. Still it should already be noted here that the field dependence of the diffusion barriers is rather small, upon a change of the electric field by 0.1 V/Å the diffusion barriers change by less than 1.5 meV. Upon increasing the slab thickness to nine layers (see Fig. 1b), first of all the Li self-diffusion barrier on Li(100) is decreased from 142 meV to 125 meV showing that the slab thickness still has some influence on the barrier heights[54]. However, now the agreement in the electric field dependence of the diffusion barriers between the explicit calculations and the first-order expression is even better. This indicates that when quantum size effects due to the small thickness of the slab leading to charge oscillations are reduced [53,55–57], obviously the first-order expression of the
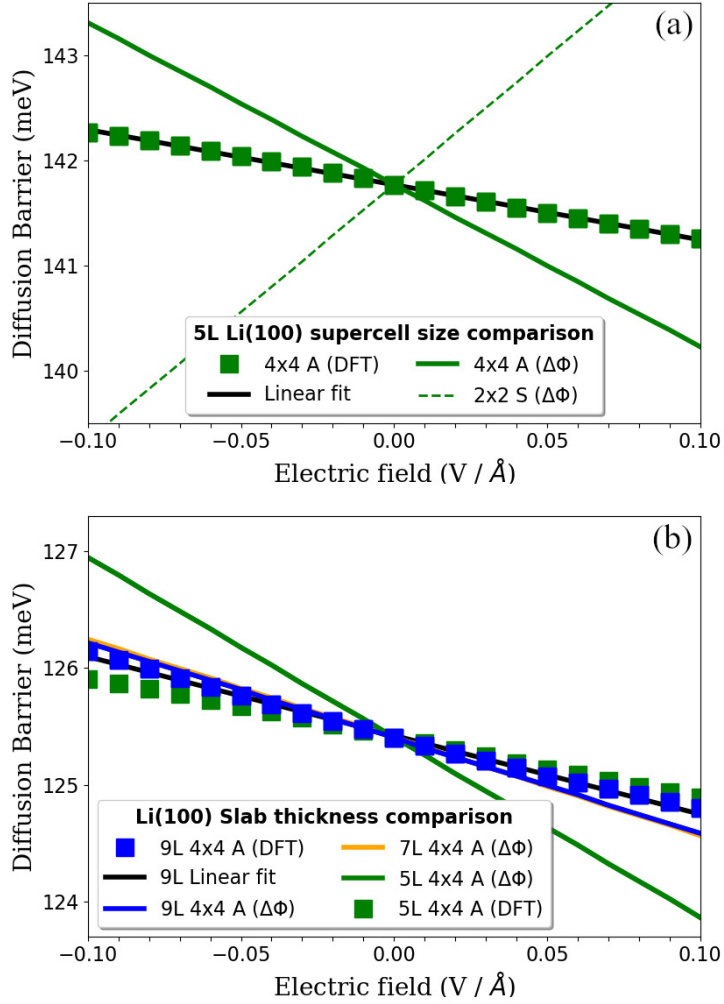
FIG. 1. Convergence of the calculations of Lithium self-diffusion in an electric field as a function of the size of the surface unit cell (panel a) and the slab thickness, i.e., the number L of layers (panel b). DFT: Diffusion barriers calculated for explicit electric fields, $\Delta\Phi$: field dependence of the diffusion barriers derived from the first-order expression Eq. 5. Note that the absolute values of the 5L and 7L results in panel b are shifted to yield the same zero-field value as the 9L results so that the slopes can be better compared.

field effects based on the work function changes becomes more appropriate. As a result of these convergence tests, in the following we only consider nine-layer slabs with a 4×4 surface unit cell to describe self-diffusion events on flat metal surfaces.

Figure 2 illustrates the calculated electric-field dependence of terrace self-diffusion barriers for the three cases, Li(100), Mg(0001) and Ag(111). In the field-free cases we obtain a barrier of 125 meV for Li(100), whereas the barrier on Mg(0001) is only about 16 meV. Hence the diffusion of Mg adatoms on Mg(0001) is much more facile than the diffusion of Li on Li(100).
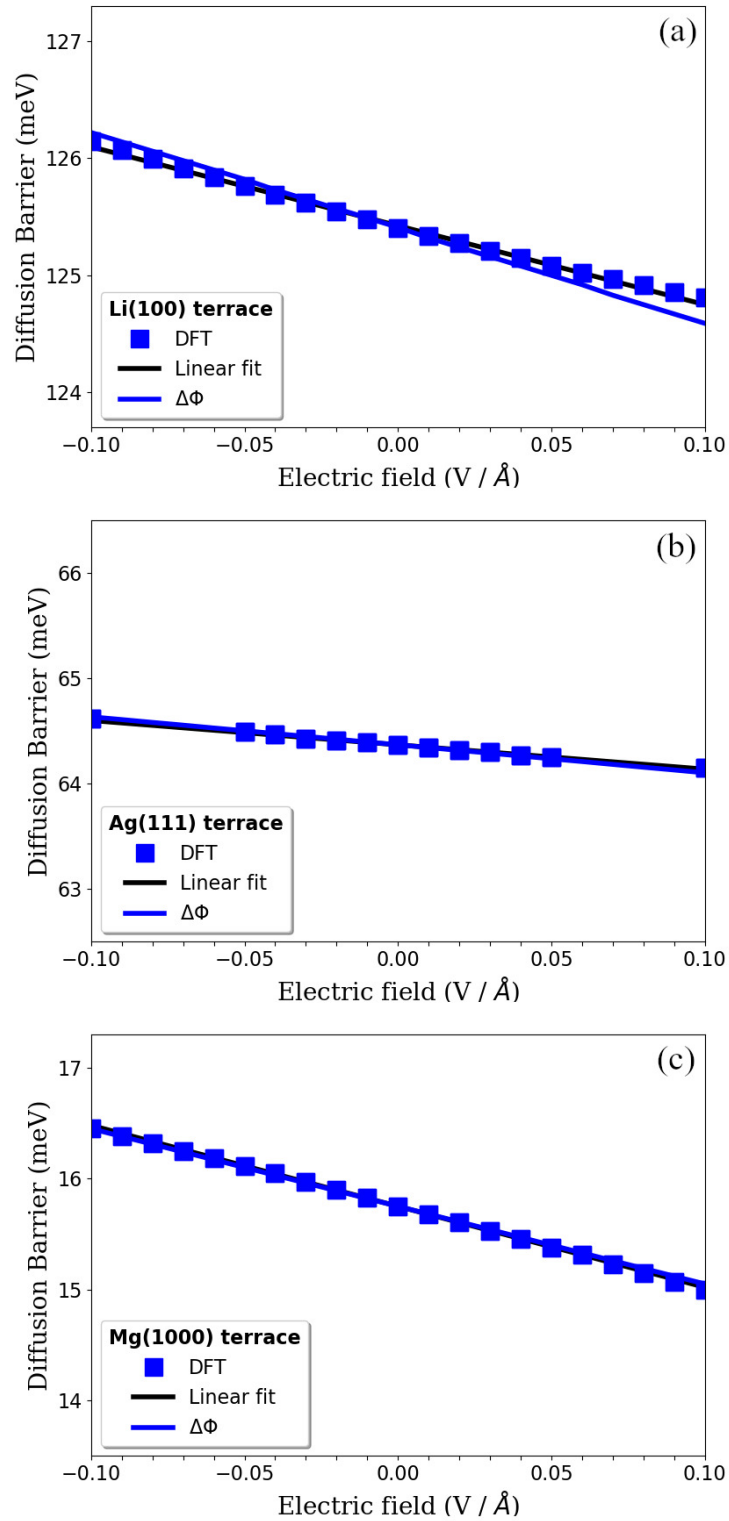
FIG. 2. Self-diffusion barriers of a) Mg/Mg(0001), b) Ag/Ag(111) and c) Li/Li(100) as a function of the electric field. DFT: Diffusion barriers calculated for different electric fields, $\Delta\Phi$: diffusion barrier function calculated via an implementation of the IST, see Eq. 5.

As mentioned above, this should lead to a much smoother growth of Mg surfaces than of Li surfaces and might explain why Mg surfaces do not tend to exhibit dendrite growth, whereas Li surfaces do. Together with the corresponding results for Na, Al, and Zn, this observation suggests that self-diffusion barriers can serve as a descriptor for dendrite growth.[16,17]

We also considered the Ag self-diffusion on Ag(111), as this is a system in which the self-diffusion has been studied before. We find a self-diffusion barrier of 64 meV which agrees well with previous calculated[58,59] and measured[60] results within the error margins.

As far as the dependence of the barriers on the electric field is concerned, in all cases the results obtained with the first-order expression (5) are in very good agreement with the calculations explicitly including the electric field. This might be surprising because electric fields of 0.1 V/Å are considered to be strong fields on a technical level[61]. However, one has to take into account that on an atomistic level the laterally averaged effective one-electron potential at metal/electrolyte interfaces varies by up to more than 10 eV/Å,[62] corresponding to local field strengths that are 100 times larger than those applied in our simulations. Hence the applied electric field indeed represents a small perturbation to the electronic structure at the surface justifying the application of first-order perturbation theory.

For all considered surfaces, we find a rather small dependence of the self-diffusion barriers on the electric field, the diffusion barriers change by only up to 0.6 meV for terrace self-diffusion on Li(100), Mg(0001) and Ag(111), as listed in Table I. In order to understand why this dependence is so weak, we have plotted in Fig. 3 the laterally averaged one-electron potential along the surface normal as determined by DFT calculations for a 5-layer Li(100) slab with explicitly applied electric fields ranging from -0.2 and 0.2 V/Å. The field strength is directly reflected by the slopes of the curves in the linear regime in the vacuum region. Figure 3 clearly demonstrates that independent of the considered field strength already 2 Å

TABLE I. Change in the self-diffusion barriers $\Delta E_{act}(|\vec{E}|)$ when an external field of $|\vec{E}| = 0.1$ V/Å is applied. T: terrace diffusion; AS: across step diffusion.

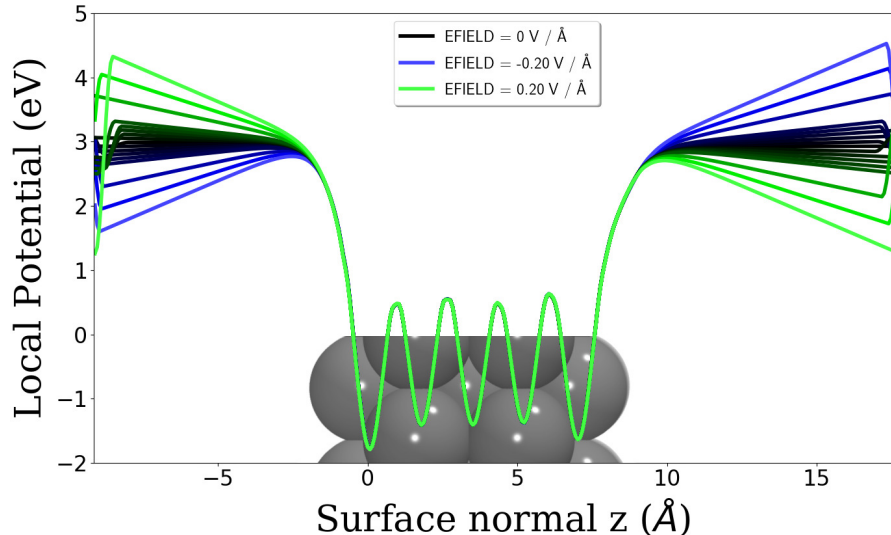| System	ΔE_{act} (meV)
Li(100) T	0.5
Mg(0001) T	0.6
Ag(111) T	0.3
Li(100) {111}-AS	3.7

8

FIG. 3. Laterally averaged one-electron potential of a Li(100) slab in the presence of electric field with field strengths between -0.2 and $0.2\,\mathrm{V/\mathring{A}}$. Note that for larger electric fields only field strengths of ± 0.1, ± 0.15 and $\pm 0.2\,\mathrm{V/\mathring{A}}$ have been included.

above the center of the uppermost Li atoms all one-electron potential curves lie above each other. This shows that also in an atomistically resolved analysis metals very effectively screen electric fields so that they can hardly penetrate, even into the surface region. These findings are also in line with the observation that atomic adsorption energies on metal surfaces depend only very weakly on an applied electric field[63].

Finally we also considered diffusion across steps. It should be noted that for three-dimensional growth in particular the diffusion barriers across steps from an upper terrace to a lower terrace are critical. If the terrace self-diffusion barrier is subtracted from these barriers, we get the so-called Schwoebel-Ehrlich barrier.[64,65] If this barrier is large, then particles deposited on some island will not propagate to the lower terrace. This then leads to a three-dimensional growth instead of a layer-by-layer growth. Interestingly enough, these barriers can be quite low[17,66] when this diffusion process occurs in the so-called exchange mechanism which is illustrated in Fig. 4. In this mechanism, which is in fact operative on Li(100) across {111} steps[17], but also on step-sites of other metal surfaces[17,66], an atom from the upper terrace replaces a step-edge atom which is pushed out onto the lower terrace. The driving force for this mechanism is the relatively high coordination of all the propagating atoms throughout the whole diffusion process. However, as the exchange mechanism involves the cooperative motion of several surface atoms, we have used the nudged elastic band (NEB)
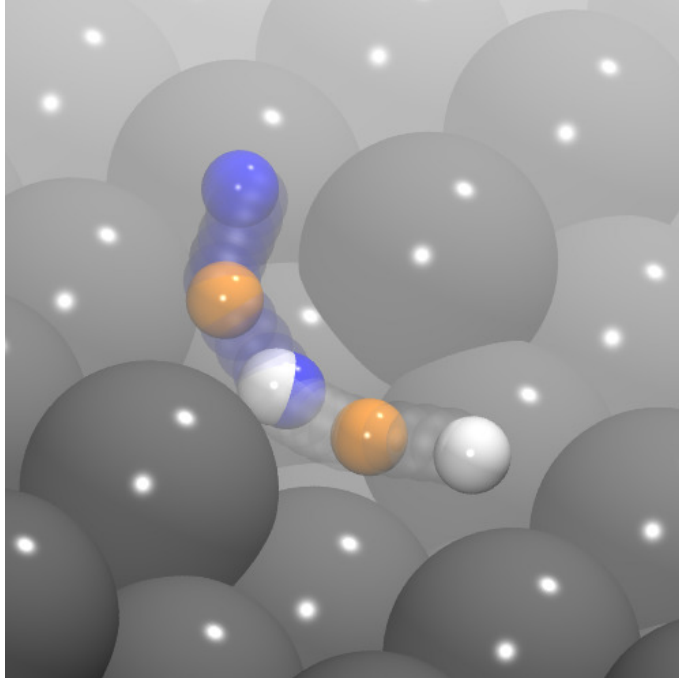
9

FIG. 4. Minimum energy path of an exchange diffusion process across a {111}-facetted step on a Li(100) surface in a field-free environment; White and blue: exchange diffusion paths for the two involved lithium atoms; Orange: transition state configurations.

method[67] that corresponds to an automatic search routine for finding the minimum energy path between specified initial and final states.

The dependence of this barrier on Li(100) for downward diffusion across a {111} step as a function of an electric field is shown in Fig. 5. First of all it needs to be mentioned that the barrier of 0.16 eV for the field-free case is somewhat lower than the barrier originally reported in our previous paper[17], but now in good agreement with another theoretical work[54]. This deviation is due to the fact that in our original determination of this particular barrier height employing the nudged elastic band (NEB) method[67] we used different cutoff parameters in the total-enery calculations for the initial and the final state on the one hand and the so-called NEB images along the minimum energy path on the other hand. Still, in spite of this quantitative adjustment all the qualitative conclusions of the previous work[17] remain valid.

The explicitly calculated change of the diffusion barriers for field strenghts of $|\vec{E}| = + 0.10$ V/Å or $|\vec{E}| = - 0.10$ V/Å is -3.4 meV and +3.7 meV, respectively. This is almost a factor of 10 larger than the corresponding dependence on the terraces (see Table I). It is probably due to the more open structure of the steps which enhances field effects. The overall field dependence is still linear and rather weak. Now the first-order expression (5) yields
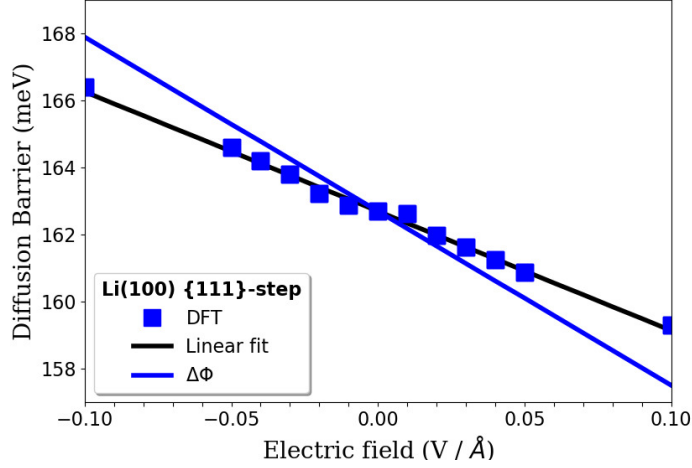
10

FIG. 5. Downward across-step diffusion barrier of a 111-facetted step on a Li(100) surface with the exchange mechanism, in dependence of an electric field. DFT: Diffusion barriers calculated for different electric fields, $\Delta\Phi$: diffusion barrier function calculated via an implementation of the IST, see eq. 5.

a slightly larger dependence of the barrier heights than the explicit DFT calculations. We obtain a change of the barrier height of $\pm\,5.2\,\mathrm{meV}$ for field strengths of $|\vec{E}| = \pm\,0.10\,\mathrm{V/\mathring{A}}$. This might again be due to the more open structure of the steps, but still the first-order expression gives an acceptable estimate of the electric-field dependence of the diffusion barrier.

Thus we find only a small influence of the electric fields on the barriers for metal for self-diffusion. Relying on the assumption that these barriers determine the intial steps of dendrite formation and thus can serve as a descriptor for dendrite growth, these initial steps on the atomistic level should not be significantly modified by the presence of electric fields. This does not mean that the process of further dendrite growth, once they reach mesoscopic or macroscopic sizes, is not significantly incluenced by the electric field strength. However, these processes basically correspond to macroscopic phenomena that depend on general metallic properties. Thus they do not discriminate between the different metals and thus can not be used to explain why some metals exhibit a strong tendency towwards dendrite growth and some not.

IV. CONCLUSIONS AND OUTLOOK

In this work, we have studied the barriers in terrace self-diffusion on Li(100), Mg(0001) and Ag(111) and downward a {111} step on Li(100) as a function of an applied external electric field. This study was motivated by our recent work showing that self-diffusion barriers could serve as a descriptor for dendrite growth in batteries. However, in the determination of the diffusion barriers, so far we had not taken into account the electrochemical environment. As a first step towards a more realistic modeling of the conditions in the electric double layer at electrode/electrolyte interfaces, we have therefore considered electric field effects by explicitly taking them into account in periodic DFT calculations, and in a first-order approximation based on the work function difference between the transition and the initial state. Both approaches yield rather similar results.

In general we find a rather weak dependence of the height of the diffusion barriers on the applied electric field which we explain by the good screening properties of metal electrodes that do not allow electric fields to effectively penetrate into the electrodes. Hence electric field effects are not likely to modify the correlation between the height of self-diffusion barriers and the likelihood for dendrite growth. Our results related to the good screening properties are not only relevant for dendrite growth, but in general for structures and processes such as adsorption at electrochemical interfaces between metal electrodes and electrolytes.

Still it should be stressed again that in this work no theory of dendrite growth has been presented. We have only confirmed that the correlation between the height of self-diffusion barriers and the occurence of dendrite-growth in batteries is still valid if electric field effects are taken into account. As the growth of dendrites occurs on mesoscopic and even macroscopic length scales, an appropriate modeling requires approaches that combine processes on macroscopic length scales with input parameters derived on the microscopic level in order to yield element-specific simulation results. This is the subject of ongoing work in our group.

---

[1] T. Kåberger, Global Energy Interconnect. **1**, 48 (2018).

[2] *Energy Statistics Pocketbook 2019*, Statistical Papers Series E No. 2 (United Nations, Department of Economic and Social Affairs: Statistics Division, 2019).

[3] F. Barbir, T. N. Veziroğlu, and H. J. Plass, Int. J. Hydrogen Energy **15**, 739 (1990).

[4] M. Hoel and S. Kverndokk, Resour. Energy Econ. **18**, 115 (1996).

[5] L. Stougie, N. Giustozzi, H. v. d. Kooi, and A. Stoppato, Int. J. Energy Res. **42**, 2916 (2018).

[6] X.-C. Wang, J. J. Klemeš, X. Dong, W. Fan, Z. Xu, Y. Wang, and P. S. Varbanov, Renew. Sustain. Energy Rev. **105**, 71 (2019).

[7] N. Mahmud and A. Zahedi, Renew. Sustain. Energy Rev. **64**, 582 (2016).

[8] S. Kakran and S. Chanana, Renew. Sustain. Energy Rev. **81**, 524 (2018).

[9] Y. Yang, S. Bremner, C. Menictas, and M. Kay, Renew. Sustain. Energy Rev. **91**, 109 (2018).

[10] Z. Li, J. Huang, B. Y. Liaw, V. Metzler, and J. Zhang, J. Pow. Sourc. **254**, 168 (2014).

[11] J. Christensen, P. Albertus, R. S. Sanchez-Carrera, T. Lohmann, B. Kozinsky, R. Liedtke, J. Ahmed, and A. Kojic, J. Electrochem. Soc. **159**, R1 (2012).

[12] W. Xu, J. Wang, F. Ding, X. Chen, E. Nasybulin, Y. Zhang, and J.-G. Zhang, Energy Environ. Sci. **7**, 513 (2014).

[13] X.-B. Cheng, R. Zhang, C.-Z. Zhao, and Q. Zhang, Chem. Rev. **117**, 10403 (2017).

[14] M. Rosso, C. Brissot, A. Teyssot, M. Dollé, L. Sannier, J.-M. Tarascon, R. Bouchet, and S. Lascaud, Electrochim. Acta **51**, 5334 (2006).

[15] X. H. Liu, L. Zhong, L. Q. Zhang, A. Kushima, S. X. Mao, J. Li, Z. Z. Ye, J. P. Sullivan, and J. Y. Huang, Appl. Phys. Lett. **98**, 183107 (2011).

[16] M. Jäckle and A. Groß, J. Chem. Phys. **141**, 174710 (2014).

[17] M. Jäckle, K. Helmbrecht, M. Smits, D. Stottmeister, and A. Groß, Energy Environ. Sci. **11**, 3400 (2018).

[18] A. Groß, Top. Curr. Chem. **376**, 17 (2018).

[19] H. Müller-Krumbhaar, M. Zimmer, T. Ihle, and Y. Saito, Physica A **224**, 322 (1996).

[20] H. Helmholtz, Ann. Phys. **165**, 211 (1853).

[21] H. Helmholtz, Ann. Phys. **165**, 353 (1853).

[22] M. Gouy, J. Phys. Theor. Appl. **9**, 457 (1910).

[23] D. L. Chapman, Philos. Mag. **25**, 475 (1913).

[24] O. Stern, Z. Elektrochem. Angew. Phys. Chem. **30**, 508 (1913).

[25] O. M. Magnussen and A. Groß, J. Am. Chem. Soc. **141**, 4777 (2019).

[26] A. Groß and S. Sakong, Curr. Opin. Electrochem. **14**, 1 (2019).

[27] K. Leung and A. Leenheer, J. Phys. Chem. C **119**, 10234 (2015).

[28] Y. Aizawa, K. Yamamoto, T. Sato, H. Murata, R. Yoshida, C. A. J. Fisher, T. Kato, Y. Iriyama, and T. Hirayama, Ultramicroscopy **178**, 20 (2017).

[29] J. O. Bockris and A. K. N. Reddy, *Modern Electrochemistry*, 1st ed. (Plenum Press, New York, 1970) p. 346.

[30] L. W. Swanson, R. W. Strayer, and F. M. Charbonnier, Surf. Sci. **2**, 177 (1964).

[31] M. P. Hyman and J. W. Medlin, J. Phys. Chem. B **109**, 6304 (2005).

[32] Z. M. Ao, S. Li, and Q. Jiang, Solid State Commun. **150**, 680 (2010).

[33] H. Ibach, M. Giesen, and W. Schmickler, J. Electroanal. Chem. **544**, 13 (2003).

[34] A. Roudgar and A. Groß, Chem. Phys. Lett. **409**, 157 (2005).

[35] F. Che, J. T. Gray, S. Ha, N. Kruse, S. L. Scott, and J.-S. McEwen, ACS Catal. **8**, 5153 (2018).

[36] Y. Guo, H. Li, and T. Zhai, Adv. Mater. **29**, 1700007 (2017).

[37] R. Davidson, A. Verma, D. Santos, F. Hao, C. Fincher, S. Xiang, J. van Buskirk, K. Xie, M. Pharr, P. P. Mukherjee, and S. Banerjee, ACS Energy Lett. **4**, 375 (2019).

[38] C. M. MacLaughlin, ACS Energy Lett. **4**, 572 (2019).

[39] E. Brener, H. Müller-Krumbhaar, D. Temkin, and T. Abel, Physica A: Statistical Mechanics and its Applications **249**, 73 (1998).

[40] H. Ghassemi, M. Au, N. Chen, P. A. Heiden, and R. S. Yassar, Appl. Phys. Lett. **99**, 123113 (2011).

[41] O. Crowther and A. C. West, J. Electrochem. Soc. **155**, A806 (2008).

[42] J. Steiger, D. Kramer, and R. Mönig, Electrochim. Acta **136**, 529 (2014).

[43] J. Steiger, D. Kramer, and R. Mönig, J. Power Sources **261**, 112 (2014).

[44] G. Kresse and J. Furthmüller, Phys. Rev. B **54**, 11169 (1996).

[45] G. Kresse and J. Furthmüller, Comput. Mater. Sci. **6**, 15 (1996).

[46] J. P. Perdew, K. Burke, and M. Ernzerhof, Phys. Rev. Lett. **77**, 3865 (1996).

[47] P. E. Blöchl, Phys. Rev. B **50**, 17953 (1994).

[48] G. Kresse and D. Joubert, Phys. Rev. B **59**, 1758 (1999).

[49] J. Neugebauer and M. Scheffler, Phys. Rev. B **46**, 16067 (1992).

[50] P. J. Feibelman, Phys. Rev. B **64**, 125403 (2001).

[51] M. Giesen, G. Beltramo, S. Dieluweit, J. Müller, H. Ibach, and W. Schmickler, Surf. Sci. **595**, 127 (2005).

[52] T. Roman and A. Groß, Phys. Rev. Lett. **110**, 156804 (2013).

[53] F. Gossenberger, T. Roman, K. Forster-Tonigold, and A. Groß, Beilstein J. Nanotechnol. **5**, 152 (2014).

[54] D. Gaissmaier, D. Fantauzzi, and T. Jacob, J. Chem. Phys. **150**, 041723 (2019).

[55] T. C. Leung, C. L. Kao, W. S. Su, Y. J. Feng, and C. T. Chan, Phys. Rev. B **68**, 195408 (2003).

[56] P. C. Rusu and G. Brocks, Phys. Rev. B **74**, 073414 (2006).

[57] J. A. Steckel, Phys. Rev. B **77**, 115412 (2008).

[58] G. Boisvert and L. J. Lewis, Phys. Rev. B **54**, 2880 (1996).

[59] C. Ratsch, A. P. Seitsonen, and M. Scheffler, Phys. Rev. B **55**, 6750 (1997).

[60] H. Brune, K. Bromann, H. Röder, K. Kern, J. Jacobsen, P. Stoltze, K. Jacobsen, and J. Nørskov, Phys. Rev. B **52**, R14380 (1995).

[61] R. G. Compton and C. E. Banks, *Understanding Voltammetry*, 2nd ed. (Imperial College Press, 2010) p. 367 ff.

[62] S. Sakong and A. Groß, J. Chem. Phys. **149**, 084705 (2018).

[63] J. K. Nørskov, J. Rossmeisl, A. Logadottir, L. Lindqvist, J. R. Kitchin, T. Bligaard, and H. Jónsson, J. Phys. Chem. B **108**, 17886 (2004).

[64] R. L. Schwoebel and E. J. Shipsey, J. Appl. Phys. **37**, 3682 (1966).

[65] G. Ehrlich and F. G. Hudda, J. Chem. Phys. **44**, 1039 (1966).

[66] X. Lin, A. Dasgupta, F. Xie, T. Schimmel, F. Evers, and A. Groß, Electrochim. Acta **140**, 505 (2014).

[67] G. Henkelman and H. Jónsson, J. Chem. Phys. **111**, 7010 (1999).